Spatial Distribution Analysis of Total Suspended Solid (TSS) using PlanetScope Data in Menjer Lake, Wonosobo Regency

Putu Wirabumi [1,*], Pramaditya Wicaksono[2], Muhammad Kamal[2], Iwan Ridwansyah[3], Luki Subehi[3], Aan Dianto[3]

[1]Masters Degree Remote Sensing Study Programs, Faculty of Geography, Gadjah Mada University, Yogyakarta, 55281, Indonesia.
[2] Department of Geographic Information Science, Faculty of Geography, Gadjah Mada University, Yogyakarta, 55281, Indonesia.
[3] Research Centre for Limnology, Indonesian Institute of Sciences, Cibinong, Bogor, 16911, Indonesia.
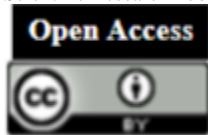*Corresponding author e-mail: wirabumiputu@gmail.com

Abstract

TSS (Total Suspended Solid) is one of the optical parameters that can be used for turbidity key indicator to assess water quality. The rapid development of remote sensing technology in the field of mapping has resulted in various methods for estimating TSS concentrations. The spatial, spectral, and temporal characteristics of PlanetScope data have the potential to estimate TSS concentrations. This study aims to determine the best method for estimating TSS concentrations and mapping the spatial distribution of TSS at a depth of 0 – 0.2 m using PlanetScope data. There are 4 single bands, 12 band ratio combinations, and 4 PC-bands in TSS mapping. Single bands, band ratio combinations, and PC-band which able to pass the significance limit of r value on the number of samples (n) are used in empirical modeling of PlanetScope data with field data using regression tests. The results show that: 1) 4 band ratio combinations (B1/B4, B2/B4, B3/B4, B4/B3) and one PC-band (PC-2) significantly correlated with TSS (mg/l), 2) PC-2 is the best spectral transformation in estimating TSS concentrations in Menjer Lake, indicated by the SE value of 3.47 mg/l with maximum accuracy produced at 78.62%, 3) all models that significantly correlated are over-estimated, indicated by the variations in model plots are below the 1:1 plot line, 4) high TSS concentrations are in the north, west, and south around the edge of the lake because of the inlets and the floating net cages, while the low concentration is in the middle of the lake.

Keywords: *TSS, Single Band, Band Ratio, PC-Band, Empirical Modeling, Standard Error of Estimate.*

1. Introduction

Total Suspended Solid (TSS) is one of the water physical parameters that can be used as a variable in monitoring water quality problems. The existence of TSS with high concentrations can disrupt the aquatic ecosystems balance which in turn adversely affects the survival of the organisms because TSS does not dissolve easily in water in a short time, causing water to become turbid. According to Kristanto (2002) turbidity indicates the optical nature of the water which results in light refraction into the body of water thus the turbidity will limit the entry of sunlight into the body of water. This can affect phytoplankton that acts as a primary producers in waters to carry out photosynthesis because of the limited light entering the body of water.

The water quality overview in monitoring is represented on the physical condition of waters which can be assessed using remote sensing technology. The spectral, spatial, and temporal characteristics owned by remote sensing data can be used to identify objects on the surface of the earth, such as TSS which is included in optical parameters in the waters. Spectral characteristics are related to the number and dimensions of wavelength intervals (band) in the electromagnetic spectrum (Jensen, 2016), spatial characteristics relate to the smallest size of an object that can be detected by remote sensing (Danoedoro, 2012), and temporal characteristics related to the system ability to perform repeating recording in the same area (Danoedoro, 2012). Remote sensing data can produce TSS information which is one of the waters physical parameters to assess water quality. TSS can be used as a water turbidity key indicator by using certain approach (Lo, 1986; Yanti *et al.*, 2016; Dhannahisvara *et al.*, 2018).

Various approaches used in mapping by utilizing remote sensing technology have been developed

over time to estimate TSS concentrations using satellite imagery. Some of these approaches can be categorized into 4 general groups (Hossain *et al.*, 2007): (1) Simple regression (correlation between single band and in-situ data. (2) Spectral unmixing technique (3) Band ratio technique by using two or more bands, and (4) Multiple regressions (using multiple bands and in-situ data). Research by Dhannahisvara *et al.*, (2018) utilized SPOT-6 data in building empirical models to estimate TSS concentrations from single band imagery, band ratio combinations, and TSS index through regression analysis with field data. Research by Yanti *et al.*, (2016) utilized Landsat 8 OLI data in TSS mapping from a single band imagery through regression analysis with field data. Research by Nurandani (2013) utilized Landsat 7 ETM + data to map the TSS distribution and built models using the band ratio technique.

Most of the algorithms used on producing information about TSS concentrations with remote sensing satellites utilize visible band and near infrared band because of the resulted correlation from in-situ measurements with imagery reflectance values can describe TSS concentrations. According to Jensen (2014) wavelengths in the visible band (0.580 - 0.690 μm) can be used to obtain information about the type of suspended sediment, whereas the near infrared wavelengths (0.714 - 0.880 μm) can be used to determine the amount of suspended sediment if the suspended sediment is the most dominant element in the water column. The use of near infrared wavelengths depends on the condition of very turbid waters where there is sufficient scattering to overcome the strong absorption at that wavelength, whereas in condition where the water level is less turbid, the suitable wavelength for building an algorithm limited to only using visible band around 665 nm (Binding *et al.*, 2005).

TSS monitoring using in-situ measurements is spatially limited, whereas using remote sensing can overcome these limitations with spatial distribution (Lee *et al.*, 2011). In the mapping context, in-situ measurements can be used to calibrate remote sensing data and assessing the accuracy (Congalton & Green, 2009; Jensen, 2016). One of the remote sensing satellite imagery, which has the spectral, spatial, and temporal characteristics that can be used for extracting TSS information is PlanetScope image. PlanetScope satellite is the latest remote sensing data product was launched in 2016. PlanetScope imagery data offers several advantages in obtaining information when sensing objects on the surface of the earth (such as TSS) and is included in the Passive Remote Sensing System. According to Planet Labs data (2019) about product specifications, the advantages of PlanetScope's imagery are having a very fast iteration time (i.e. for 1 day), carries 4 spectral bands (blue, green, red, and near infrared), and has high spatial resolution (3 m). A fast temporal resolution is expected to be able to describe the information in actual in relation between imagery recording date and in-situ measurements. Multispectral imagery (visible and near infrared bands) can be used to assess aquatic bodies condition such as TSS, phytoplankton, dissolved organic matter, and other mineral particles using remote sensing (Doxaran *et al.*, 2002). As the latest

satellites imagery product and with the several advantages owned by PlanetScope imagery, it's necessary to check how good, accurate, and can be applied, especially in TSS mapping.

This study aims to determine the best method of PlanetScope imagery in estimating TSS concentration, including 4 single band reflectances (blue, green, red, and near infrared), 12 band ratios, and 4 PC-bands (Principle Component Analysis) and mapping the TSS spatial distribution based on the best method.

2. Methods

2.1 Data

PlanetScope satellites have 98° inclination angle with altitude of 475 km which is located in sun-synchronous orbit and has 24.6 km x 16.4 km frame size. With that orbit, PlanetScope satellites will do the recording in the morning and afternoon, especially the equator at 09:30 - 11:30 am and capable of recording 20,000 km^2 area for 1 day at-nadir (Planet Labs, 2019).

PlanetScope satellite imagery product used in this study was Level 3A PlanetScope Ortho Tile products imagery recorded on October 25, 2019 where the imagery product had been corrected geometrically to the orthorectification level, had been radiometrically corrected to the level of BoA (Bottom of Atmosphere) reflectance, and had UTM (Universal Transverse Mercator) projection. PlanetScope imagery carries 4 multispectral bands, namely blue band (455 - 515 nm), green band (500 - 590 nm), red band (590 - 670 nm), and near infrared band (780 - 860 nm). PlanetScope imagery has a spatial resolution of 3 m, very fast temporal resolution (1 day), and 12-bit radiometric resolution.

2.2 Study Sites

This research was conducted in Menjer Lake, Maron Village, Garung District, Wonosobo Regency, Central Java, Indonesia. Menjer Lake has a geographical position at the center of the lake at 7°16 'SL and 109° 55' EL. According to LIPI (2019) Menjer Lake is located at an altitude of 1300 meters above sea level, belonged in Dieng Plateau topography which has steep relief. The area of the lake is around 70 Ha, has a maximum water depth of ± 52 m with an average water depth of ± 17.5 m. The land use in northern, eastern, and western side of the lake are dominated by plantations and forests, while in the southern side is dominated by agricultural land and settlements. Menjer Lake gets its water from 3 sub-watersheds, which are Menjer water catchment area, Serayu upstream, and Klakah sub-watershed. Menjer Lake is used to collect water as a Hydroelectric Power Plant. The water from the Klakah Dam is flowed into Serayu River and then through the Serayu Dam it's flowed through the Klakah Tunnel (Serayu) to Menjer Lake. In addition, Menjer Lake is also used for inland fisheries (floating net cages), agriculture, tourism, and irrigation (LIPI 2019). The research location is shown in Figure 1.
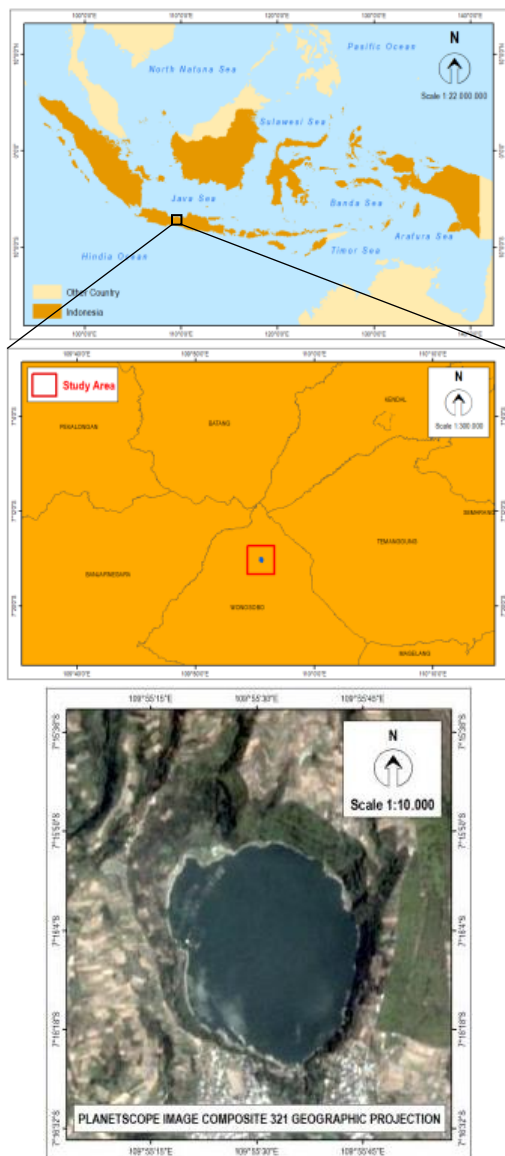
Fig 1. Research Location at Menjer Lake, Wonosobo Regency, Central Java, Indonesia

2.3 Single and Spectral Transformation Bands

The spectral transformation method used in this study includes: 4 single bands (B1/blue band, B2/green band, B3/red band, B4/near infrared band), 12 band ratio combinations, and 4 PC-bands PCA (Principle Component Analysis) results (Table 1).

The changes in pixel values could be caused by the material addition in the water column. The single band method utilizes attenuation or weakening of energy propagating in the water column characterized by increasing depth (relating to energy penetration in penetrating waters) thus the energy is getting smaller and the longer the wavelengths is the much stronger it is being attenuated compared to shorter wavelengths (Bukata *et al.*, 1995; Goodman *et al.*, 2013; Wicaksono, 2015).

Band ratio are usually used to produce certain effects in its relation with protruding the spectral aspects (appearance variation of certain objects) with reference to the object spectral reflectance curve on which the method is performed (Danoedoro, 2012).

PCA is a rotation technique that being applied to a multi-channel coordinate system thus producing a new imagery with a smaller number of bands with a clearer pixel value distribution in presenting the appearance of objects thus efficient in visual imagery observation and multispectral classification process without reducing the information content (Danoedoro, 2012).

Table 1. Single and Spectral Transformation Bands

Inputs	Algorithm
Single Band	B1, B2, B3, B4
Band Ratio	B1/B2, B1/B3, B1/B4, B2/B1, B2/B3, B2/B4, B3/B1, B3/B2, B3/B4, B4/B1, B4/B2, B4/B3
PCA	PC-1, PC-2, PC-3, PC-4

2.4 Field Survey

The field survey was carried out on October 28, 2019. The water samples taken were TSS suspended at water depths of 0 - 0.2 m. The determination of field survey points based on the transect method. The specified transects could represent other areas. The field survey was divided into 2: measurement and water sampling. The field measurements aimed to obtain turbidity values (FTU) using the RINKO-Profiler Conductivity Temperature Depth (CTD) ASTD 152 tool from the results of the calculation average turbidity value that obtained at a depth of 0 m and 0.2 m. The tool is able to measure and record several parameters in the waters in a vertical measurement (can reach up to 600 m deep). The parameters that can be measured using these tools are turbidity, chlorophyll-a, dissolved oxygen (DO), salinity, conductivity, temperature, and water depth (Table 2).

Table 2. Sensor Spesification RINKO-Profiler ASTD 152

Parameter	Principal	Range	Resolution	Accuracy	Time Constant
Depth	Semiconductor Pressure Sensor	0 to 600 m or 0 to 1000 m	0 to 600 m (range 0.02 m) or 0 to 1000 m (range 0.03 m)	±0.3% FS	0.2 s
Temperature	Thermistor	-3 to 45°C	0.001°C	±0.01°C (0 to 35°C)	0.2 s
Conductivity	Electrode	0.5 to 70 mS cm^{-1}	0.001 mS cm^{-1}	±0.01 mS cm-1	0.2 s
Salinity	Practical Salinity	2 to 42	0.001	-	0.2 s
DO	Phosphore scene	0 to 20 mg L^{-1} (0 to 200)%	0.01% (0.01 mg L^{-1})	±2% FS	0.4 s
Chlorophyll	Fluorimeter	0 to 400 ppb (Uranine reference)	0.01 ppb	±1% FS Zero drift ±0.1 ppb	0.2 s
Turbidity	Backscattering	0 to 1000 FTU (Formazin reference)	0.03 FTU	±0.3 FTU or measured value ±2%	0.2 s

The water sampling in the field aimed to calibrate the turbidity data (FTU) into TSS concentration data (mg / l). The water samples were taken using the Niskin Water Sampler. The water sample was then laboratory tested using gravimetric methods as in the standard water analysis method to obtain TSS concentration values (mg / l). 29 sample points (shown in Figure 2) were obtained in the field survey where 18 sample points were used for empirical

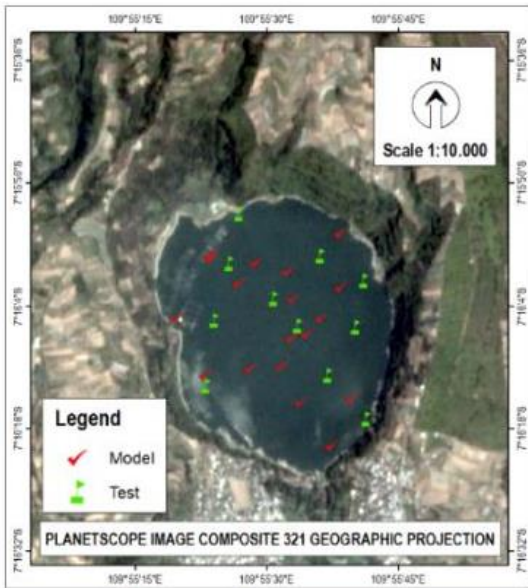modeling and 11 sample points were used for accuracy testing.

Fig 2. Distribution Sample Models and Tests

2.5 TSS Mapping

The empirical modeling began with data normality test with Kolmogorov-Smirnov, correlation analysis with Pearson Product Moment Bootstrapp technique, regression analysis with linear and non-linear regression (exponent, logarithmic, 2nd Order Polynomial, and power. The significance level for the statistical analysis used was 95% (Wicaksono, 2015; Dhannahisvara et al, 2018).

Kolmogorov-Smirnov Function:
$$Dn = IF_T - F_S I \quad …………......…………….. \quad (1)$$

Pearson Product Moment Function:
$$r = \frac{n \sum x_i y_i - \sum x_i y_i}{\sqrt{n \sum xi^2 - (\sum xi)^2} \cdot \sqrt{n \sum yi^2 - (\sum yi)^2}} \quad ….... \quad (2)$$

Linear Regression Function:
$$y = a + bx \quad …………...……..……..… \quad (3)$$

Exponent Regression Function:
$$y = ae^{bx} \quad …………………......…….... \quad (4)$$

Logarithmic Function:
$$y = a \ln(x) + b \quad ………....……………. \quad (5)$$

2nd Order Polynomial Regression Function:
$$y = a_0 + a_1 X^1 + a_2 X^2 \quad ….....……….... \quad (6)$$

Power Regression Function:
$$y = ax^b \quad ……………………………… \quad (7)$$

Data normality test performed because this research is included in parametric statistic and the data must be normally distributed. Correlation analysis performed to determine the relationship between PlanetScope data which in this case the imagery pixel value from the single band and spectral transformation with TSS field data to obtain the correlation coefficient value (r). The single band and spectral transformation that passed the significance limit of r value on the number of samples (n) and had a significant relationship with field TSS was used as an input in empirical modeling through regression analysis. The regression analysis used were linear

and non-linear regression (exponential, logarithmic, polynomial order 2, and power). The regression analysis produced the determination coefficient (R^2) and the resultant regression function. The determination coefficient describes how much the dependent variable (field TSS) can be explained or predicted by the independent variable (PlanetScope imagery pixel value) in a regression model. The resultant regression function from regression analysis of each band was used to convert the PlanetScope imagery pixel value into TSS concentration value in mg/l units through band math (Wicaksono, 2015; Dhannahisvara et al, 2018).

2.6 Accuract Assessment

Accuracy assessment was carried out on each TSS model to determine and / or assess how much error from the model was, based on reference test data. The accuracy assessment calculation results can show how well the model quality to be applied. The accuracy assessment used was the Standard Error of Estimate (SE) (Asdak, 2002). The samples that being used for accuracy assessment were the samples that not being used in modeling, which were as many as 11 samples. The SE values indicate deviations between the model data with reference data and can be under-estimate or over-estimate which can be indicated by a 1:1 plot line. The best TSS model which can be used to predict TSS concentrations is seen from how big the accuracy maximum percentage is and how low the SE value is.

3. Results and Discussion

3.1 Empirical Modelling

Based on the Kolmogorov-Smirnov normality test shown in table 2, TSS samples with a total of 18 data have a result of Dn = 0.14. The normality test results interpretation is if the data normally distributed then Dn < Ks table and if the data is not normally distributed then Dn > Ks table. The normality test result shows that the data are normally distributed where Dn < Ks table (0.14 < 0.32) and thus those 18 data samples can proceed for further analysis. Correlation analysis is used to determine the relationship between field data (TSS) and imagery data (imagery pixel values). The data is significantly correlated if r count > r table where r table from 18 number of samples (n) is 0.468 with a significance level of 95%. Based on table 3, the input which significantly correlated and passes using Bootstrapp technique are 4 band ratio combinations (B1/B4, B2/B4, B3/B4, B4/B3) and one PC-band (PC-2). In other words, that significant spectral transformation can be used as input in TSS modeling through regression analysis. The highest correlation is obtained from PC-2 input with r = 0.544 and the lowest is B2/B4 with r = 0.492. There is a negative r value from the correlation analysis results which means the increasing in spectral reflectance is followed by the TSS concentration produced getting lower.

Wirabumi *et al*.,/ JAGI Vol 4 No 1/2020

Table 2. Normality test using Kolmogorov-Smirnov

Statistics	Var
N Sample	18
Mean	13,60
Standard Deviation	3,38
Dn	0,14
KS Table (0,05)	0,32

Table 3. Correlation analysis with Bootstrapp technique

Input	r	Input	r
B1	-0,274	B3/B1	0,142
B2	-0,142	B3/B2	-0,029
B3	-0,129	B3/B4*	-0,512
B4	0,411	B4/B1**	0,489
B1/B2	-0,233	B4/B2**	0,486
B1/B3	-0,145	B4/B3*	0,504
B1/B4*	-0,494	PC1	-0,057
B2/B1	0,235	PC2*	0,544
B2/B3	0,025	PC3	-0,129
B2/B4*	-0,492	PC4	-0,109

*significant at 95%CL and comply bootstrapp correlation
**significant at 95%CL but not comply bootstrapp correlation

TSS modeling input is a single and spectral transformation bands that correlates significantly to field TSS data. The regression analysis model performed were linear and non-linear regression which included exponent, logarithmic, second order polynomials, and power. On PC-2, logarithmic and power non-linear regression models couldn't be performed because there were several pixel values that contained negative values. Based on table 4, it shows that the highest and consistent determination (R^2) coefficient value on all significant spectral transformation inputs is by the non-linear regression model second order polynomial even though the determination value produced between linear and non-linear regression has a not significant difference. There are several factors that can influence this, one of which is the complexity of the material suspended in the water column. The material complexity in the water column causes the reflectance value to be varied in responding the object because many are caused by the scattering and the absorption in the suspended material water, thus the determination value generated based on the sample distribution pattern by using linear regression becomes weak.

It can be said that the wavelength characteristics being used particularly the visible band (both single band, band ratio originating from the combination of several visible bands, and PCA), material suspended in the water column, and water depth become the main factors why the linearity between imagery pixel values and field TSS is difficult to explain. Non-linear regression model gives higher R^2 values than linear regression model because of its ability to follow a more flexible sample distribution pattern between the imagery pixel values and field TSS. Scatter plots from the linear and the non-linear regression model of each of the spectral transformations are shown in figures 3 - 7.

Table 4. Regression analysis using linear and non-linear

| Model	Resultant Regression Function	R^2
PC-2		
Linear	121,79x + 13,814	0,296
Exponent	13,386e^{8,6238x}	0,2493
2nd Order Polynomial	-866,53x² + 142,52x + 14,039	0,3031
B3/B4		
Linear	-15,111x + 37,939	0,2618
Exponent	75,377e^{-1,082x}	0,2255
Logarithmic	-22,98ln(x) + 24,495	0,2588
2nd Order Polynomial	-5,9054x² + 3,1073x + 23,989	0,2629
Power	28,748x^{-1,644}	0,2225
B4/B3		
Linear	34,443x - 7,8964	0,2539
Exponent	2,837e^{2,4615x}	0,2178
Logarithmic	22,977ln(x) + 24,495	0,2588
2nd Order Polynomial	-85,448x² + 148,42x - 45,554	0,2635
Power	28,748x^{1,6441}	0,2225
B1/B4		
Linear	-8,3029x + 34,85	0,2437
Exponent	59,354e^{-0,588x}	0,2051
Logarithmic	-20,19ln(x) + 32,511	0,2419
2nd Order Polynomial	-1,5382x² - 0,7321x + 25,607	0,2443
Power	50,216x^{-1,428}	0,2032
B2/B4		
Linear	-9,938x + 36,184	0,2421
Exponent	65,532e^{-0,706x}	0,205
Logarithmic	-21,5ln(x) + 31,188	0,2399
2nd Order Polynomial	-2,8508x² + 2,5483x + 22,606	0,2432
Power	45,888x^{-1,524}	0,2026
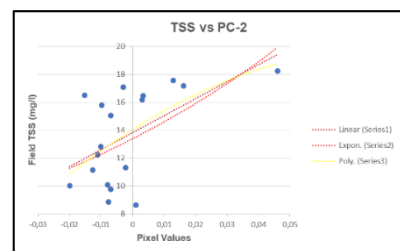
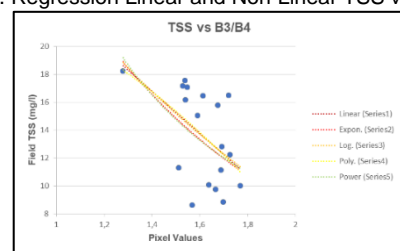Fig 3. Regression Linear and Non-Linear TSS vs PC-2

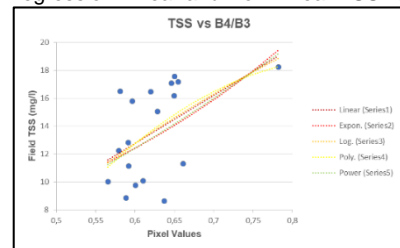Fig 4. Regression Linear and Non-Linear TSS vs B3/B4

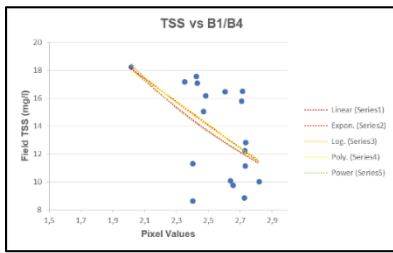Fig 5. Regression Linear and Non-Linear TSS vs B4/B3
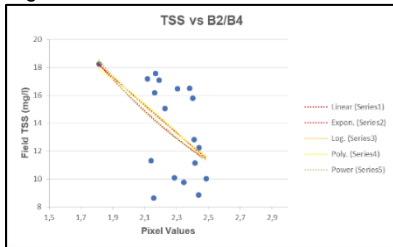
Fig 6. Regression Linear and Non-Linear TSS vs B1/B4

Fig 7. Regression Linear and Non-Linear TSS vs B2/B4

The resultant regression function of each TSS regression model is used as input in converting pixel values to TSS in mg/l units in PlanetScope imagery. Accuracy assessment will be conducted next on the values that are already in mg/l units from each model. Accuracy assessment was conducted to determine the errors deviations from the generated model. Furthermore, accuracy assessment is also used to determine the best model for mapping. TSS at Menjer Lake uses PlanetScope data because the generated R^2 value only explains how strong the relationship between pixel values and TSS is and how explainable TSS variations are by imagery pixel values. The model can be underestimate and / or overestimate seen from the 1:1 plot line between the reference data (field) and the model data. The accuracy assessment conducted in this study was using the Standard Error of Estimate (SE). The best model is indicated with the lowest SE value (mg/l) and highest maximum accuracy (%). Based on table 5, empirical modeling of PC-2 using exponential non-linear regression models has the highest level of accuracy when compared to other models. The generated SE value was 3.47 mg/l and the maximum accuracy was 78.62%. The SE value indicates that there is a difference of ± 3.47 mg/l between the modeling results TSS value from PC-2 and the actual TSS value in the field. Based on figures 8 - 12, the overall empirical model is over-estimate as indicated by the model data variation over the field data (reference data) which is dominant below the 1:1 plot line.

Table 5. Accuracy assessment results

Model	SE (mg/l)	Maximum Accuracy (%)
PC-2		
Linear	3,58	77,92
Exponent**	3,47	78,62*
2nd OrderPolynomial	3,69	77,27
B3/B4		
Linear	3,61	77,77
Exponent	3,52	78,29
Logarithmic	3,6	77,84
2nd OrderPolynomial	3,61	77,74
Power	3,52	78,3*
B4/B3		
Linear	3,58	77,94
Exponent	3,51	78,34*
Logarithmic	3,6	77,84
2nd OrderPolynomial	3,63	77,63
Power	3,52	78,31
B1/B4		
Linear	3,81	76,52
Exponent	3,74	76,96*
Logarithmic	3,84	76,36
2nd OrderPolynomial	3,79	76,66
Power	3,79	76,64
B2/B4		
Linear	3,85	76,3
Exponent	3,79	76,66*
Logarithmic	3,88	76,08
2nd OrderPolynomial	3,8	76,55
Power	3,87	76,18

*highest accuracy assesment for each inputs spectral transformation
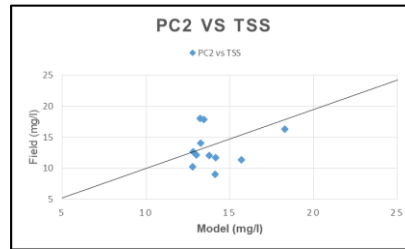**best empirical modelling for estimated concentration of TSS (mg/l)

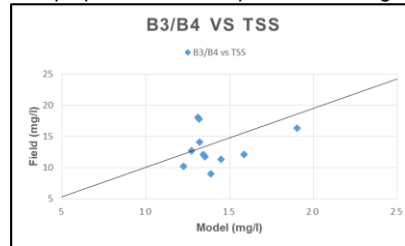Fig 8. Graph plot 1:1 from empirical modelling of PC-2

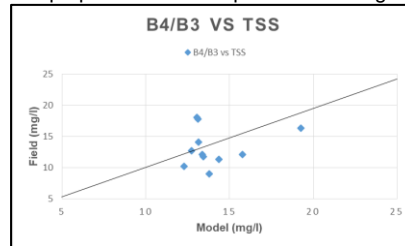Fig 9. Graph plot 1:1 from empirical modelling of B3/B4

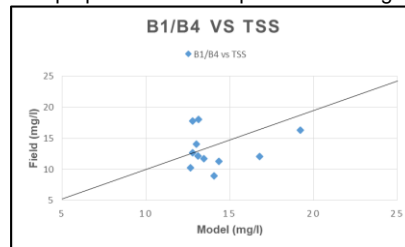Fig 10. Graph plot 1:1 from empirical modelling of B4/B3

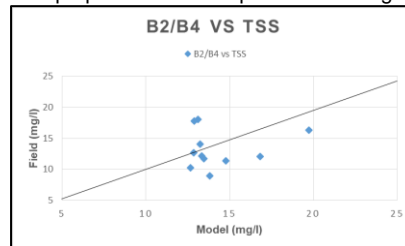Fig 11. Graph plot 1:1 from empirical modelling of B1/B4

Fig 12. Graph plot 1:1 from empirical modelling of B2/B4

Based on the accuracy assessment result, empirical modeling that has high accuracy rate and consistent with all spectral transformation input is by

using exponential non-linear regression model from PC-2, B4/B3, B1/B4, and B2/B4 while in the combination band B3/B4 is using the power model. Sequentially the highest to lowest accuracy obtained from the PC-2 empirical model (exponential non-linear regression; 3.47 mg/l; 78.62%), B4/B3 (exponential non-linear regression; 3.51 mg/l; 78.34%), B3/B4 (non-linear power regression; 3.52 mg/l; 78.3%), B1/B4 (exponential non-linear regression; 3.74 mg/l; 76.96%), and B2/B4 (exponential non-linear regression; 3.79 mg/l; 76.66%). However, the difference in accuracy values between each model is not too large where the SE value overall difference is only 0.1 mg/l and the maximum accuracy is only 0.1%, its shows that empirical modeling by using all significant spectral transformation input and by using linear and non-linear regression models in general can be used in Menjer Lake TSS mapping.

PC-2 input has the highest accuracy value and is the best model in Menjer Lake TSS mapping compared to the band ratio combination. This can occur because of the spectral transformation by using PCA is able to highlight hidden information that cannot be displayed by ordinary spectral band. PCA rotates data to produce new bands with a small amount but has special and unique information on each band (Smith, 2005; Murti & Wicaksono, 2014). Furthermore, PCA is able to minimize noise on the single band imagery and noise is usually placed on the last PC-band (Wicaksono, 2014). It also shows that in this study a single band from PlanetScope imagery used as an spectral transformation input does not contribute to Menjer Lake TSS mapping because there are a lot of noise on a single band imagery which causes the information contained in single band to be disrupted which is being proved in the absence of a correlation between a single band with actual TSS data in the field.

The presence of significant correlation between the band ratio combinations with the actual field TSS data in Menjer Lake also answers the existing theory that band ratio combinations can highlight certain responses from objects in the waters based on the spectral reflectance curve of the object. The band ratio combinations contain a lot of information in the red and near infrared bands. According to Doxaran et al., (2002) when TSS concentrations are low the significant correlation is using band ratios. The dominance of band ratio over significant correlations indicates that in this study at Menjer Lake the TSS concentrations are included in the low levels. The TSS spatial distribution in Menjer Lake from each modeling input that has high accuracy value is shown in Figure 13.

3.2 Spatial Distribution of TSS

Based on the results of the TSS spatial distribution mapping with a scale of 1: 5,000 on each of the empirical modeling inputs that significantly correlated show that TSS concentrations in Menjer Lake ranged between 9 - 29 mg/l. The TSS spreads from high concentrations at the edge of the lake and low concentrations in the middle of the lake. Five classes were obtained in Menjer Lake TSS mapping using equal interval classification methods. Menjer Lake is dominated by water with TSS content between 9 - 21 mg/l (class 1 to class 3). High TSS

concentrations are on the northern, western and southern banks. In the northern and southern part there are water inlets from the Serayu watershed that enter the lake through a tributary, the high TSS concentration can be caused by the materials that carried by the flow of water entering through the inlet. Whereas in the western part of the lake there is a floating net cage and a tourism ship dock, the high TSS concentration in that part is caused by the suspended nutrient originating from fish feed around the floating net cage area that enters the body of the water. Moreover, the TSS distribution pattern in Menjer Lake has a high concentration equally dominant on the edge of the lake, another indication is caused by the soil erosion carried into the body of water and suspended in the waters because of the TSS is not easily to dissolve quickly and cannot settle directly in the waters in a short time.
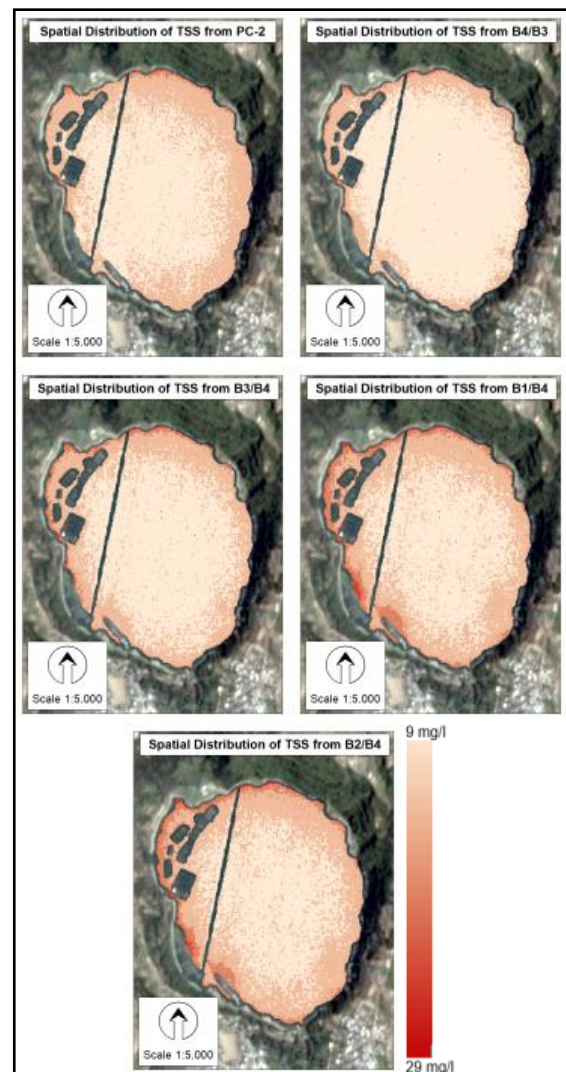

Fig 13. Spatial Distribution of TSS

Based on the calculation of the total estimated TSS concentration using the best input model, PC-2 at Menjer Lake is 1.26 tons with assumption that the total estimated TSS concentration generated is based on the suspended TSS in the water column with a depth of 0 - 0.2 m. On average, each of the water sampling at a depth of 0 - 0.2 m produced 13.37 mg/l TSS concentrations from the PC-2 model input.

4. Conclusion

The spectral transformation method from PCA and the band ratio combinations can be used as a model in TSS mapping while the single band from PlanetScope data contribute less on the TSS mapping in Menjer Lake. The best spectral transformation input in mapping the TSS spatial distribution in Menjer Lake using PlanetScope data is PC-2, the SE value results is 3.47 mg/l and the maximum accuracy is 78.62%. The value on the PC-band is very dependent on pixel values variation in the imagery scene therefore it's scene-dependent, the application at different locations can have different results. The band ratio combinations of B4/B3 produces a maximum accuracy of 78.34%, B3/B4 produces 78.30%, B1/B4 produces 76.96%, and B2/B4 produces 76.66%. The all models that significantly correlated have an over-estimate tendency. The estimated total of TSS concentrations using the model with the highest accuracy is 1.26 tons. The high concentrations of TSS distribution in Menjer Lake is located in the northern, western, and the southern precisely at the edge of the lake, while the TSS distribution begins to decrease in the middle of the lake area.

Acknowledgements

References

Asdak, C. (2002). Hidrologi dan Pengelolaan Daerah Aliran Sungai. Gajah Mada University Press, Yogyakarta.

Binding, C. E., Bowers, D. G., & Mitchelson Jacob, E. G. (2005). Estimating Suspended Sediment Concentrations from Ocean Colour Measurements in Moderately Turbid Waters: The Impact of Variable Particle Scattering Properties. Remote Sensing of Environment, 94: 373-383.

Bukata, R. P., Jerome, J. H., Kondratyev, K. Y., & Pozdnyakov, D. V. (1995). Optical Properties and Remote Sensing of Inland and Coastal Waters. NY: CRC, 362p.

Congalton, R. G., & Green, K. (2009). Assessing the Accuracy of Remotely Sensed Data: Principle and Practice. Boca Raton: Taylor & Francis Group.

Danoedoro, Projo. (2012). Pengantar Penginderaan Jauh Digital. Yogyakarta: ANDI Yogyakarta.

Dhannahisvara, A. J., Hartono., Wicaksono, P., & Nugroho, F. S. (2018). Total Suspended Solid Distribution Analysis Using SPOT-6 Data in Segara Anakan Cilacap. Journal of Geomatics and Planning, 5(2), 177-188.

Doxaran, D., Froidefond, J. M., Lavender, S., & Castaing, P. (2002). Spectral Signature of Highly Turbid Waters: Application with SPOT Data to Quantify Suspended Particulate Matter Concentrations. Remote Sensing of Environment, 81: 149-161.

Effendi, Hefni. (2003). Telaah Kualitas Air Bagi Pengelolaan Sumber Daya dan Lingkungan Perairan. Yogyakarta: Kanisius.

Goodman, J. A., Purkis, S. J., & Phinn, S. R. (2013). Corel Reef Remote Sensing A Guide for Mapping, Monitoring and Management. (S. R. Phinn, Ed.) Springer.

Hossain, A. K., Jia, Y., & Chao, X. (2007). Development of Remote Sensing Based Index for Estimating/Mapping Suspended Sediment Concentration in River or Lake Environments. Mississipi: ResearchGate.

Jensen, J.R. (2014). Remote Sensing of the Environment an Earth Resource Perspective. Second Edition. England: Pearson New International Edition.

Jensen, J.R. (2016). Introductory Digital Image Processing: A Remote Sensing Perspective. 4th Edition. USA: Pearson Education.

Kristanto, P. (2002). Ekologi Industri. Yogyakarta: ANDI.

Lee, M. S., Park, K. A., Chung, J. Y., Ahn, Y. H., & Moon, J. E. (2011). Estimation of Coastal Suspended Sediment Concentration Using Satellite Data and Oceanic Insitu Measurement. Korean Journal of Remote Sensing, 27(6), 677-692.

Lembaga Ilmu Pengetahuan Indonesia (LIPI). (2019). Studi Daya Tampung, Daya Dukung, dan Zonasi Telaga Menjer PLTA Garung Unit Pembangkitan Mrica. Pusat Penelitian Limnologi (P2L).

Lo, C. P. (1986). Penginderaan Jauh Terapan. Diterjemahkan oleh: Bambang Purbowaseso. Jakarta: UI Press.

Murti, H. S., & Wicaksono, P. (2014). Analisis Saluran Spektral Yang Paling Berpengaruh Dalam Identifikasi Kesehatan Terumbu Karang: Studi Kasus Pulau Menjangan Besar dan Menjangan Kecil, Kepulauan Karimunjawa. Majalah Ilmiah Globe, Desember 2014, 16(2), 117-124.

Nurandani, P., Subiyanto, S., & Sasmito, B. (2013). Pemetaan Total Suspended Solid (TSS) menggunakan Citra Satelit Multitemporal di Danau Rawa Pening Provinsi Jawa Tengah. Jurnal Geodesi UNDIP, 2 (4), 72-84.

Planet Labs. (2019). Planet Imagery Product Specification. Planet Labs Inc 2019.

Smith, R.B. (2005). Outline of Principle Component Analysis. Site: https://yceo.yale.edu/sites/default/files/files/PCA_Outline.pdf. (Accessed 20.7.19).

Wicaksono, P. (2014). Pemetaan Makro Alga Menggunakan Citra Penginderaan Jauh Resolusi Spasial Tinggi di Pulau Kemujan

Kepulauan Karimunjawa. Seminar Nasional Teknologi Terapan II. Sekolah Vokasi UGM. Yogyakarta.

Wicaksono, P. (2015). Perbandingan Akurasi Metode Band Tunggal dan Band Rasio untuk Pemetaan Batimetri pada Laut Dangkal Optis. Simposium Nasional Sains Geoinformasi IV. 802-810.

Yanti, A., Susilo, B., & Wicaksono, P. (2016). The Aplication of Landsat 8 OLI for Total Suspended Solid (TSS) Mapping in Gajahmungkur Reservoir Wonogiri Regency. International Conference of Indonesian Society for Remote Sensing (ICOIRS). 47(1), p. 012028.